

EVOLUTION KERNELS FOR PARTON SHOWER MONTE CARLO*

A. KUSINA

Laboratoire de Physique Subatomique et de Cosmologie
Université Grenoble-Alpes, CNRS/IN2P3
53 avenue des Martyrs, 38026 Grenoble, France

O. GITULIAR, S. JADACH, M. SKRZYPEK

The Henryk Niewodniczański Institute of Nuclear Physics
Polish Academy of Sciences
Radzikowskiego 152, 31-342 Kraków, Poland

(Received June 16, 2015)

We report on re-calculation of the next-to-leading order DGLAP evolution kernels performed in a scheme suited for Monte Carlo simulations of parton cascades (parton showers).

DOI:10.5506/APhysPolB.46.1343

PACS numbers: 12.38.-t, 12.38.Bx, 12.38.Cy

1. Introduction

In this contribution, we report on the calculation of the next-to-leading order (NLO) DGLAP evolution kernels that was started in Refs. [1, 2]. The inclusive DGLAP splitting functions at NLO have been known for a long time, they were first calculated in early 1980s [3–6]. Today also the next-to-next-to-leading order (NNLO) corrections have been known for over ten years [7, 8] so why there is the interest in NLO splitting functions? The reason for this is the fact that all the above mentioned calculations were performed in the $\overline{\text{MS}}$ scheme and by their nature are inclusive. A direct motivation for the current work comes from Monte Carlo simulations of parton cascades in a form of parton shower (PS) generators. In particular, from the effort of the Cracow group that aims to include full NLO corrections

* Presented by A. Kusina at the Cracow Epiphany Conference on the Future High Energy Colliders, Kraków, Poland, January 8–10, 2015.

in the parton shower simulations [9–12]. This means not only corrections to the hard matrix element, as is done in approaches like MC@NLO [13] and POWHEG [14], but also the full NLO corrections to the parton cascades.

The big difficulty with including NLO corrections in parton shower algorithms is connected with the nature of parton shower generators. Specifically, in PS approach, all the subsequent parton emissions need to be treated in fully exclusive way, meaning that their 4-momenta are not integrated (including transverse degrees of freedom). For comparison, in a standard inclusive QCD calculations there are two elements, Wilson coefficient (parton level hard matrix element) and parton distribution functions (PDFs) that sum up all the above mentioned emissions in an inclusive way. Moreover, if we go beyond LO in PS approach, we need additional prescription to avoid double counting of contributions in hard matrix element and in the shower. This is referred to as the NLO matching and it was a major improvement for PS in the last decade. It was originally done with MC@NLO method and shortly after the POWHEG method was introduced. Recently, an alternative solution from the Cracow group is also available referred to as KrkNLO method [12]. This new solution is distinct from the earlier methods in a number of ways, one of them being the use of different factorization scheme. Instead of using traditional $\overline{\text{MS}}$ scheme that was designed for simplicity of inclusive calculations, this method uses a dedicated factorization scheme, referred to as Monte Carlo (MC) scheme, which was designed especially for Monte Carlo simulations of parton cascades. The purpose of introducing this scheme was not only NLO matching but rather simplification of a more difficult task that is including NLO corrections in the shower and maybe even later matching of the NLO shower with an NNLO matrix element. One of the necessary ingredients needed for this purpose are NLO evolution kernels calculated in the MC scheme. We first calculated the real emission corrections to the non-singlet NLO splitting functions [1] as these were required for proof of concept of the methodology to include NLO corrections in the shower [9, 10]. Recently, we complemented the scheme by providing prescriptions for computing virtual corrections and also calculated them for the non-singlet case [2]. Currently, we are finishing the calculation of the NLO splitting functions and in this contribution, we are reporting on the progress.

2. Monte Carlo friendly regularization scheme

The regularization prescription for computing NLO splitting functions is one of the ingredients of the Monte Carlo factorization scheme [12]. It is based on the prescription of Curci, Furmanski and Petronzio (CFP) introduced in [5] during the first NLO kernel calculation in x space. The

most important features of the CFP scheme are: (i) the use of axial gauge; and (ii) principal value (PV) regularization for the axial gluon propagators [leading to infrared (IR) singularities], namely

$$g^{\mu\nu} - \frac{l^\mu n^\nu + l^\nu n^\mu}{ln} \rightarrow g^{\mu\nu} - \frac{l^\mu n^\nu + l^\nu n^\mu}{[ln]_{\text{PV}}}, \quad \frac{1}{[ln]_{\text{PV}}} = \frac{ln}{(ln)^2 + \delta^2(pl)}, \quad (1)$$

where n is the axial gauge vector, p is an external reference momentum and δ is the PV geometrical regulator. Unfortunately, the use of PV prescription in this way leads to complicated patterns for cancellation of singularities between real and virtual diagrams, which is unacceptable if we want to use them for the construction of PS Monte Carlo.

We illustrate it on the example of the non-singlet diagram NLO-qq-d displayed in Fig. 1. If calculated using CFP ($\overline{\text{MS}}$) prescription, the virtual graph gives (we provide here only the singular terms)

$$\begin{aligned} \Gamma_{\text{NLO-qq-d}}^{\text{virt PV}} &\sim \frac{1}{\epsilon^3} [-p_{qq}(x)] \\ &+ \frac{1}{\epsilon^2} \left[p_{qq}(x) \left(-6I_0 - 2\ln(1-x) - \ln(x) + \frac{3}{2} \right) + (1-x) \right] \\ &+ \frac{1}{\epsilon} [p_{qq}(x) (-2I_1 + 6I_0 \ln(1-x) + 2I_0 \ln(x)) + 6(1-x)I_0], \quad (2) \end{aligned}$$

and the corresponding real graph reads

$$\begin{aligned} \Gamma_{\text{NLO-qq-d}}^{\text{real PV}} &\sim \frac{1}{\epsilon^3} [p_{qq}(x)] + \frac{1}{\epsilon^2} [p_{qq}(x) (2I_0) - (1-x)] \\ &+ \frac{1}{\epsilon} [p_{qq}(x) (-2I_1 + 4I_0 - 2I_0 \ln(1-x) + 2I_0 \ln(x)) - 2(1-x)I_0], \quad (3) \end{aligned}$$

where $p_{qq}(x) = \frac{1+x^2}{1-x}$ is the LO qq kernel, and I_0 and I_1 represent single and double logarithmic singularities regulated by the PV regulator δ

$$\begin{aligned} I_0 &= \int_0^1 dx \frac{1}{[x]_{\text{PV}}} = -\ln \delta + \mathcal{O}(\delta), \\ I_1 &= \int_0^1 dx \frac{\ln x}{[x]_{\text{PV}}} = -\frac{1}{2} \ln^2 \delta - \frac{\pi^2}{24} + \mathcal{O}(\delta). \quad (4) \end{aligned}$$

We can see that higher order ϵ poles cancel between the corresponding real and virtual graphs, which is probably impossible to implement in a MC shower program.

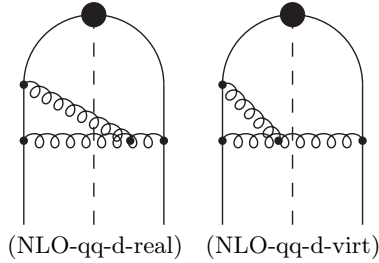


Fig. 1. Selected non-singlet diagrams contributing to the P_{qq} kernel.

Because of this fact, we have modified the CFP prescription by changing the way PV regularization is applied. Instead of applying it only to the gluon propagators, we apply it to all the singularities in the plus variable, $l^+ = nl/np$, see [2]. This results in simplification of the real–virtual cancellations which can be seen by examining results for NLO-qq-d graphs in the new prescription (referred as NPV). The virtual graph is given by

$$\Gamma_{\text{NLO-qq-d}}^{\text{virt NPV}} \sim \frac{1}{\epsilon^2} \left[p_{qq}(x) \left(-4I_0 - 2\ln(1-x) - \ln(x) + \frac{3}{2} \right) \right] + \frac{1}{\epsilon} [p_{qq}(x) (-6I_1 + 6I_0 \ln(1-x) + 2I_0 \ln(x)) + 4(1-x)I_0], \quad (5)$$

and the real graph is

$$\Gamma_{\text{NLO-qq-d}}^{\text{real NPV}} \sim \frac{1}{\epsilon} [p_{qq}(x) (2I_1 + 4I_0 - 2I_0 \ln(1-x) + 2I_0 \ln(x))]. \quad (6)$$

One can easily check that adding real and virtual graphs in both prescriptions leads to the same final results. However, from the MC point of view, the situation in the NPV prescription is hugely improved. There are no triple ϵ poles, the double poles occur only in the virtual graph and the real one is free of them¹.

Actually, a general statement is valid². In the case of the NPV regularization: (i) ϵ^3 poles in virtual and real graphs are absent (replaced by $1/\epsilon \ln^2 \delta$ -type structures), and (nearly) all ϵ^2 poles originate from the virtual graphs alone, (ii) all real emission graphs (contributing to NLO splitting functions) feature only single ϵ poles, (iii) sum of real and virtual graphs for the same topology reproduces the corresponding sum calculated using CFP prescription.

¹ More specifically, the $1/\epsilon^3$ terms have been replaced by $1/\epsilon \ln^2 \delta$ -type terms, regulated simultaneously by ϵ and δ .

² With some exceptions related to running of the coupling constant and CFP projection operators.

There are some additional subtleties connected to the graphs contributing to the running of the strong coupling (*e.g.* NLO-gg-f), these are partly discussed in Ref. [2].

Using NPV regularization prescription is the first step on the way to the results in the Monte Carlo scheme. For the MC shower simulations, we need purely 4-dimensional calculations and, as we can see above, the presented results still feature single (and partly double) ϵ poles. This can be, however, avoided by introducing additional cut-off regularization for the overall scale integration. It was already done in [1] when we calculated real emission contributions to the non-singlet splitting functions and will not be discussed here.

3. Status of the calculation

Currently, we are finishing the calculation of the singlet splitting functions using the prescription described in the previous section and introduced in [1, 2]. At the moment, we have recalculated the full P_{gg} and P_{gg} kernel on the inclusive level and we have obtained a perfect agreement with the literature. Below, we present the inclusive “parton density” (defined as in [15]) for the case of P_{gg} . It is obtained as a sum of contributions from individual diagrams in Fig. 2

$$\begin{aligned}
 \Gamma_{gg} = & \frac{C_A^2}{2\epsilon} \left(\frac{\alpha_S}{2\pi}\right)^2 \left\{ \frac{1}{\epsilon} \left[p_{gg}(x) \left(\frac{11}{3} - 8I_0 - 8\ln(1-x) - 4\ln(x) \right) \right. \right. \\
 & + \frac{44}{3} \left(\frac{1}{x} - x^2 \right) - 12(1-x) + 8(1+x)\ln(x) \left. \right] + 2p_{gg}(-x)S_2(x) \\
 & + p_{gg}(x) \left(\ln^2(x) - 4\ln(x)\ln(1-x) - \frac{\pi^2}{3} + \frac{67}{9} \right) + 4(1+x)\ln^2(x) \\
 & - \left. \left(\frac{44}{3}x^2 - \frac{11}{3}x + \frac{25}{3} \right) \ln(x) + \frac{27}{2}(1-x) + \frac{67}{9} \left(x^2 - \frac{1}{x} \right) \right\} \\
 & + \frac{C_A T_f}{2\epsilon} \left(\frac{\alpha_S}{2\pi}\right)^2 \left[\left(-\frac{8}{3} \frac{1}{2\epsilon} - \frac{20}{9} \right) p_{gg}(x) + \frac{26x^2}{9} - 2x + 2 - \frac{26}{9x} \right. \\
 & \left. - \frac{4}{3}(1+x)\ln(x) \right] \\
 & + \frac{C_F T_f}{2\epsilon} \left(\frac{\alpha_S}{2\pi}\right)^2 \left[\frac{1}{2\epsilon} \left(4x - 4 - \frac{16}{3} \frac{1-x^3}{x} - 8(1+x)\ln(x) \right) \right. \\
 & \left. + \frac{20x^2}{3} + 8x - 16 + \frac{4}{3x} - 2(1+x)\ln^2(x) - (10x+6)\ln(x) \right], \quad (7)
 \end{aligned}$$

where

$$p_{gg}(x) = \frac{(1-x+x^2)^2}{x(1-x)}, \tag{8}$$

$$S_2(x) = \int_{\frac{x}{1+x}}^{\frac{1}{1+x}} \frac{dz}{z} \ln\left(\frac{1-z}{z}\right). \tag{9}$$

The kernel is now easily extracted from Γ_{gg} by taking twice its residue (twice as we use $n = 4 + 2\epsilon$); additionally, we exclude factor $(\frac{\alpha_S}{2\pi})^2$ which is the usual convention, then

$$\begin{aligned} P_{gg}^{(1)} &= 2 \operatorname{Res}(\Gamma_{gg}) / \left(\frac{\alpha_S}{2\pi}\right)^2 \\ &= C_A^2 \left[p_{gg}(x) \left(\ln^2(x) - 4 \ln(x) \ln(1-x) - \frac{\pi^2}{3} + \frac{67}{9} \right) \right. \\ &\quad + 2p_{gg}(-x)S_2(x) + 4(1+x) \ln^2(x) - \left(\frac{44}{3}x^2 - \frac{11}{3}x + \frac{25}{3} \right) \ln(x) \\ &\quad \left. + \frac{27}{2}(1-x) + \frac{67}{9} \left(x^2 - \frac{1}{x} \right) \right] \\ &\quad + C_A T_f \left[-\frac{20}{9}p_{gg}(x) + \frac{26x^2}{9} - 2x + 2 - \frac{26}{9x} - \frac{4}{3}(1+x) \ln(x) \right] \\ &\quad + C_F T_f \left[\frac{20x^2}{3} + 8x - 16 + \frac{4}{3x} - 2(1+x) \ln^2(x) - (10x+6) \ln(x) \right]. \end{aligned} \tag{10}$$

This result reproduces the well known P_{gg} kernel that can be found in Ref. [16] or in the original Furmanski and Petronzio paper [6]. The literature provides the single ϵ terms defining the splitting functions but some of the double pole terms from the inclusive densities can also be cross-checked with the results in [17].

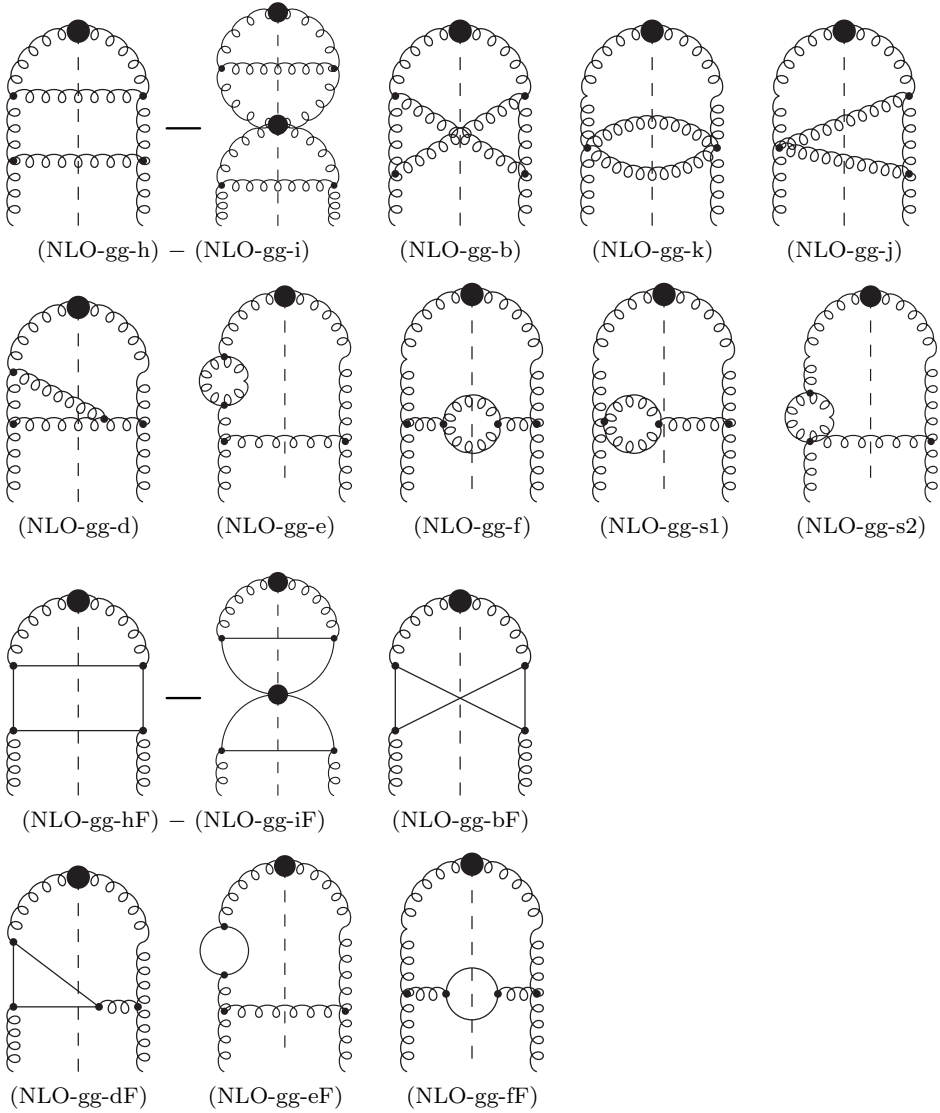


Fig. 2. List of diagrams contributing to the P_{gg} kernel. The graphs d, f, s1, dF and fF contribute in two versions, depending on the location of the cut.

Similarly for the case of P_{qg} , the inclusive density is given by (the contributing diagrams are listed in Fig. 3)

$$\begin{aligned}
 \Gamma_{qg} = & \frac{C_F T_f}{2\epsilon} \left(\frac{\alpha_S}{2\pi}\right)^2 \left\{ \frac{1}{2\epsilon} \left[p_{qg}(x) (-16I_0 - 8 \ln(1-x) - 8 \ln(x) + 12) \right. \right. \\
 & - 4(1-2x) \ln(x) - 8x + 2 \left. \right] + p_{qg}(x) \left[2 \ln^2(1-x) + 2 \ln^2(x) \right. \\
 & - 4 \ln(x) \ln(1-x) - 4 \ln(1-x) + 4 \ln(x) - \frac{2\pi^2}{3} + 10 \left. \right] \\
 & - (1-2x) \ln^2(x) - (1-4x) \ln(x) + 4 \ln(1-x) - 9x + 4 \left. \right\} \\
 & + \frac{C_A T_f}{2\epsilon} \left(\frac{\alpha_S}{2\pi}\right)^2 \left\{ \frac{1}{2\epsilon} \left[p_{qg}(x) \left(-8 \ln(1-x) + \frac{62}{3} \right) + \frac{28x}{3} - \frac{74}{3} - \frac{16}{3x} \right. \right. \\
 & - (32x+8) \ln(x) \left. \right] + p_{qg}(x) \left[-2 \ln^2(1-x) - \ln^2(x) + 4 \ln(1-x) \right. \\
 & + \frac{44}{3} \ln(x) + \frac{\pi^2}{3} - \frac{218}{9} \left. \right] + 2p_{qg}(-x)S_2(x) + \frac{14x}{9} + \frac{40}{9x} + \frac{182}{9} \\
 & - (8x+2) \ln^2(x) - \left(\frac{38}{3} - \frac{136x}{3} \right) \ln(x) - 4 \ln(1-x) \left. \right\}, \tag{11}
 \end{aligned}$$

where $p_{qg}(x) = x^2 + (1-x)^2$ is the corresponding LO kernel. The resulting splitting function is equal to

$$\begin{aligned}
 P_{qg}^{(1)} = & 2 \text{Res}(\Gamma_{qg}) / \left(\frac{\alpha_S}{2\pi}\right)^2 \\
 = & C_F T_f \left[p_{qg}(x) \left(2 \ln^2(1-x) + 2 \ln^2(x) - 4 \ln(x) \ln(1-x) - 4 \ln(1-x) \right. \right. \\
 & + 4 \ln(x) - \frac{2\pi^2}{3} + 10 \left. \right) - (1-2x) \ln^2(x) - (1-4x) \ln(x) + 4 \ln(1-x) \\
 & - 9x + 4 \left. \right] + C_A T_f \left[p_{qg}(x) \left(-2 \ln^2(1-x) - \ln^2(x) + 4 \ln(1-x) \right. \right. \\
 & + \frac{44}{3} \ln(x) + \frac{\pi^2}{3} - \frac{218}{9} \left. \right) + 2p_{qg}(-x)S_2(x) + \frac{14x}{9} + \frac{40}{9x} + \frac{182}{9} \\
 & - (8x+2) \ln^2(x) - \left(\frac{38}{3} - \frac{136x}{3} \right) \ln(x) - 4 \ln(1-x) \left. \right], \tag{12}
 \end{aligned}$$

which agrees with the literature [6, 16].

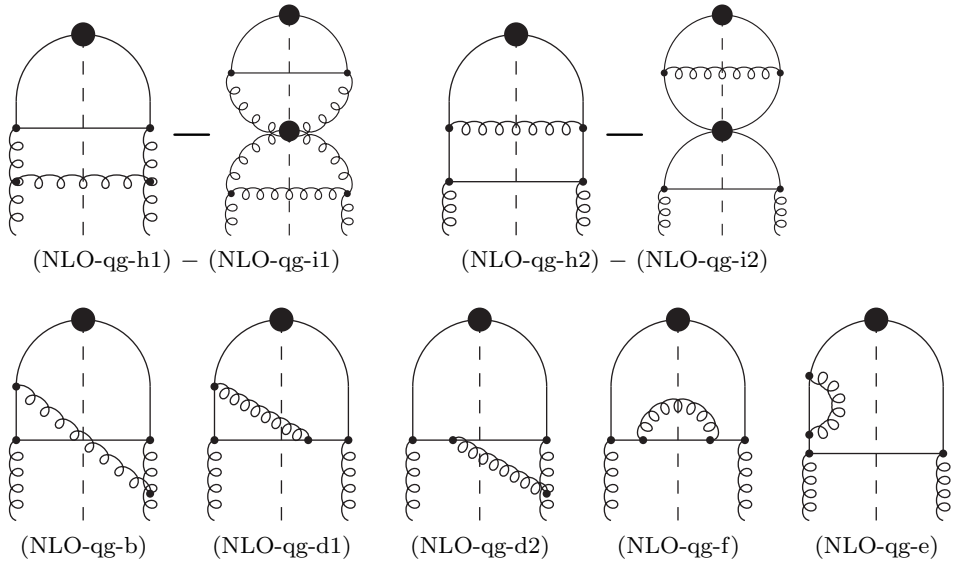


Fig. 3. List of diagrams contributing to the P_{qg} kernel. The graphs d1, d2 and f contribute in two versions, depending on the location of the cut.

The double ϵ pole terms in the inclusive densities Γ originate from two sources. The first is building up of the running coupling constant, the second is artificial and connected with the subtraction defined through the projection operator (\mathbb{P} in CFP [5]), entering via countergraphs like NLO-qg-i1 or NLO-gg-i. In the inclusive calculations, the higher ϵ poles are not important as splitting functions do not depend on them (they are defined by the residue — single pole part), making this kind of projection operator perfectly well suited for the inclusive computation. However, if we want to use the unintegrated distributions (exclusive version of Γ) in the Monte Carlo program this will become a problem. We can solve it by using a dedicated Monte Carlo factorization scheme [9, 12] which redefines projection operators, however, this is beyond the scope of this work and we will not investigate it here. Let us just mention that similar idea has been investigated by Oliveira *et al.* [18, 19] in the context of physical factorization scheme allowing for better convergence of perturbative series.

Currently, we are working to complete the calculation for P_{gq} and $P_{q\bar{q}}$ kernel. Diagrams contributing to these calculations can be seen in Figs. 4 and 5. Computation for P_{gq} is analogical to the one for P_{qq} . In the case of $P_{q\bar{q}}$, the first (Born) level contributions appear only at the order of $\mathcal{O}(\alpha_s^2)$ making this calculation very easy.

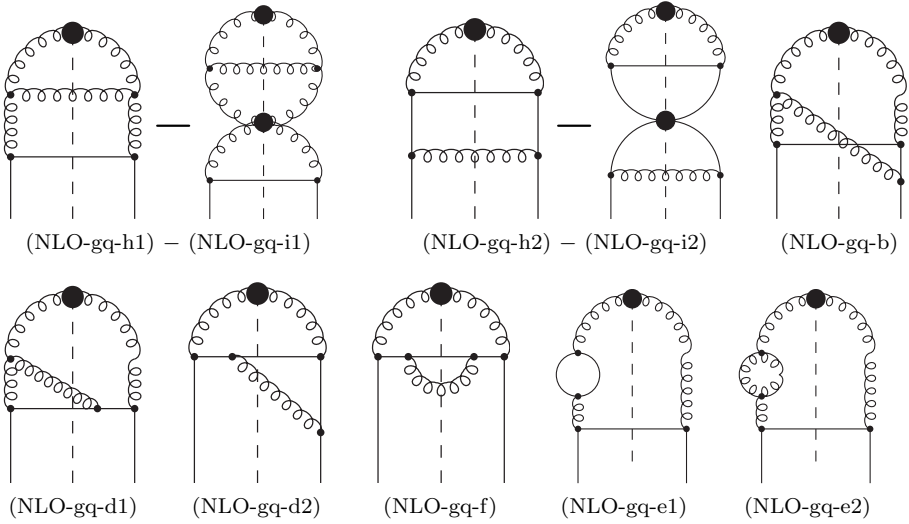


Fig. 4. List of diagrams contributing to the P_{gq} kernel. The graphs d1, d2 and f contribute in two versions, depending on the location of the cut.

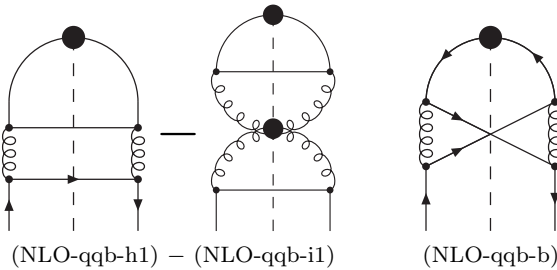


Fig. 5. List of diagrams contributing to the $P_{q\bar{q}}$ kernel.

4. Summary

We have reported on the progress of re-calculation of the NLO splitting function using new NPV regularization prescription [2]. We have already calculated the P_{gg} and P_{qg} (and earlier P_{qq}) NLO splitting functions and we have reproduced the known inclusive results from the literature. The calculations for the P_{gq} splitting function are already advanced and the partial results we have obtained so far are also in agreement with the literature.

The inclusive results presented here are *not* our main interest and serve us mainly as a cross-check of our calculations. The main interest for us are the unintegrated distributions in the new scheme that will be better suited for the Monte Carlo simulations. These distributions will be presented elsewhere.

This work has been partly supported by the Polish National Science Center grants DEC-2011/03/B/ST2/02632 and UMO-2012/04/M/ST2/00240. The work of O.G. has been supported by the Polish National Science Center with the Sonata Bis grant DEC-2013/10/E/ST2/00656.

REFERENCES

- [1] S. Jadach, A. Kusina, M. Skrzypek, M. Slawinska, *J. High Energy Phys.* **1108**, 012 (2011) [arXiv:1102.5083 [hep-ph]].
- [2] O. Gituliar, S. Jadach, A. Kusina, M. Skrzypek, *Phys. Lett. B* **732**, 218 (2014) [arXiv:1401.5087 [hep-ph]].
- [3] E.G. Floratos, D.A. Ross, C.T. Sachrajda, *Nucl. Phys. B* **129**, 66 (1977).
- [4] E.G. Floratos, D.A. Ross, C.T. Sachrajda, *Nucl. Phys. B* **152**, 493 (1979).
- [5] G. Curci, W. Furmanski, R. Petronzio, *Nucl. Phys. B* **175**, 27 (1980).
- [6] W. Furmanski, R. Petronzio, *Phys. Lett. B* **97**, 437 (1980).
- [7] S. Moch, J.A.M. Vermaseren, A. Vogt, *Nucl. Phys. B* **688**, 101 (2004) [arXiv:hep-ph/0403192].
- [8] A. Vogt, S. Moch, J.A.M. Vermaseren, *Nucl. Phys. B* **691**, 129 (2004) [arXiv:hep-ph/0404111].
- [9] S. Jadach, M. Skrzypek, A. Kusina, M. Slawinska, *PoS RADCOR2009*, 069 (2010) [arXiv:1002.0010 [hep-ph]].
- [10] M. Skrzypek *et al.*, *Acta Phys. Pol. B* **42**, 2433 (2011) [arXiv:1111.5368 [hep-ph]].
- [11] S. Jadach *et al.*, *Phys. Rev. D* **87**, 034029 (2013) [arXiv:1103.5015 [hep-ph]].
- [12] S. Jadach *et al.*, arXiv:1503.06849 [hep-ph].
- [13] S. Frixione, B.R. Webber, *J. High Energy Phys.* **0206**, 029 (2002) [arXiv:hep-ph/0204244].
- [14] P. Nason, *J. High Energy Phys.* **0411**, 040 (2004) [arXiv:hep-ph/0409146].
- [15] O. Gituliar, arXiv:1403.6897 [hep-ph].
- [16] R.K. Ellis, W. Vogelsang, arXiv:hep-ph/9602356.
- [17] G. Heinrich, *Improved Techniques to Calculate Two-loop Anomalous Dimensions in QCD*, Ph.D. Thesis, Swiss Federal Institute of Technology, Zurich 1998.
- [18] E. Oliveira, A. Martin, M. Ryskin, *Eur. Phys. J. C* **73**, 2534 (2013) [arXiv:1305.6406 [hep-ph]].
- [19] E. Oliveira, A. Martin, M. Ryskin, *J. High Energy Phys.* **1311**, 156 (2013) [arXiv:1310.8289 [hep-ph]].